J Mol Model (2011) 17:377–381
DOI 10.1007/s00894-010-0738-0

ORIGINAL PAPER

The effect of Li^+ on GSK-3 inhibition: Molecular dynamics simulation

Hao Sun · Yong-jun Jiang · Qing-sen Yu · Cheng-cai Luo · Jian-wei Zou

Received: 9 September 2009 / Accepted: 28 April 2010 / Published online: 16 May 2010

Abstract Glycogen synthase kinase-3 (GSK-3) is a kind of serine-threonine protein kinase. It places important roles in several signaling pathways and it is a key therapeutic target for a number of diseases, such as diabetes, cancer, Alzheimer's disease and chronic inflammation. Mg^{2+} ions which interact with ATP are conserved in GSK. They are important in phosphoryl transfer. Li^+ is an inhibitor for GSK-3. It is used to treat bipolar mood disorder. This paper illustrates the effect of Li^+ on GSK-3. When Mg_I^{2+} is replaced by Li^+, the atom fluctuation of GSK-3 will rise, and the in-line phosphoryl transfer mechanism is probably demolished and the binding of pre-phosphorylated substrates may be disturbed. All the results we obtained clearly suggest that inhibition to GSK-3 is caused by the Mg_I^{2+} replacement with Li^+.

Keywords Dynamic simulation · GSK-3 · Inhibitor · Lithium · Metal ions

Introduction

Glycogen synthase kinase-3 (GSK-3) is a kind of serine-threonine protein kinase. It was originally identified in 1980 and was initially shown to phosphorylate and inactivate glycogen synthase (GS), the rate-limiting enzyme of glycogen biosynthesis [1]. GSK-3 is ubiquitously expressed in eukaryotes [2, 3]. There are two major isoforms of GSK-3 in mammals: GSK-3β and GSK-3α, which are encoded by different genes. The kinase domain sequences of the two isoforms are almost the same and the main differences occur at the N and C termini [4–6].

GSK-3 plays an essential role in many different pathways. Initially GSK-3 was shown to be important in the Insulin/IGF1 and Wnt/Shaggy signaling pathways. However, recent studies reveal that GSK-3 is present in many other pathways, such as NGF signaling, Estradiol signaling, and the Reelin pathway [7]. GSK-3 is one of the most promising drug targets for adult onset type 2 diabetes, stroke, neurodegenerative disorders (Alzheimer's disease), bipolar disorder, schizophrenia acute inflammatory processes, cancer, and so forth.

So far, more than 40 substrates of GSK-3 have been discovered, and the number is still growing [8]. GSK-3 phosphorylates its substrates by recognizing the canonical phosphorylation motif SXXXpS. The motif features Ser or Thr at position P0, and a phospho-serine or phospho-threonine at position P+4. The primed phosphorylation on position P + 4 requires phosphorylation by a kinase other than GSK-3 [9]. Many kinases have two Mg^{2+}, for instance PKA and CDKs, and the two Mg^{2+} behave in different ways. MgI (the Mg^{2+} binding with β-and γ-phosphates of ATP) was generally identified as a catalytic activator, while MgII (the Mg^{2+} binding with α- and γ-phosphates of ATP) as an inhibitor [10].

Lithium has been a primary therapeutic agent for bipolar mood disorder since 1949 [11], although people did not know its inhibition on GSK-3 until 1996 [12]. Lithium can selectively inhibit GSK-3 [13, 14]. The inhibition could be influenced by the concentration of magnesium [15].

H. Sun · Y.-j. Jiang (✉) · Q.-s. Yu · C.-c. Luo · J.-w. Zou
Key Laboratory for Molecular Design and Nutrition Engineering of Ningbo City, Ningbo Institute of Technology,
Zhejiang University,
Ningbo, Zhejiang Province 315100, People's Republic of China
e-mail: yjjiang@nit.zju.net.cn

H. Sun
Southwest Forestry College,
Kunming, Yunnan Province 650224, People's Republic of China

Q.-s. Yu
Department of Chemistry, Zhejiang University,
Hangzhou, Zhejiang Province 310027,
People's Republic of China

Experiments have shown that lithium did not compete with ATP and substrates of GSK-3, but competed with Mg^{2+}, suggesting the existence of two Mg^{2+} binding sites (one is Li-sensitive and the other is Li-insensitive) [15, 16]. Ryves and Harwood proposed that Li^{+} and Mg^{2+} had similar ionic radiis, 0.60 and 0.65 angstrom respectively. This enabled Li^{+} to physically invade the low affinity Mg^{2+} binding site and subsequently disrupted the catalytic function of GSK-3 [15, 16].

To reveal how lithium inhibits GSK-3β, we performed computational studies on GSK-3β using molecular mechanical methods. We set up three enzyme complexes. One contained two Mg^{2+} ions, one contained Mg_I^{2+}(the Mg^{2+} binding with β-and γ-phosphates of ATP) while Mg_{II}^{2+} (the Mg^{2+} binding with α- and γ-phosphates of ATP) was replaced by Li^{+}, and one contained Mg_{II}^{2+} while Mg_I^{2+} was replaced by Li^{+}.

Computational methods

Preparation of the systems

The structure of GSK-3β in a complex with ATP mimic AMP-PNP (PDB code: 1PYX) was chosen as the initial structure. Absent residues on the disordered loop (residue 120 to 124 and residue 287 to 290) of the crystal structure were added and the conformations of the residues were modeled using the Loop Search module of Sybyl6.8 (Tripos Inc.). The structure of AMP-PNP was changed to that of ATP by replacing the nitrogen atom N3B in 1PYX with an oxygen atom. Three systems were prepared. System1, complex-2 Mg, featured GSK-3β with ATP and two Mg^{2+} ions. System 2, complex-LiII, featured GSK-3β with ATP and Mg_I^{2+}, while Mg_{II}^{2+} was replaced with Li^{+}. System 3, complex-LiI, featured GSK-3β with ATP and Mg_{II}^{2+}, while Mg_I^{2+} was replaced with Li^{+}.

Molecular dynamics simulations

Molecular dynamics simulations were carried out on the three systems respectively, using the SANDER module of AMBER 9.0 with the Amber FF03 and GAFF force field. The parameters of ATP, provided by Amber web site [17]. All simulations were carried out at neutral pH. Lys and Arg residues were positively charged, while Asp and Glu residues were negatively charged. The default His protonation state in AMBER_9 was adopted. Seven counterions (Cl^{-}) were added into complex-2 Mg, while six counterions (Cl^{-}) were added into complex-LiI and complex-LiII to maintain the electroneutrality of the systems. Every system was immersed in a 10 Å truncated octahedron periodic water box, and the structures of water molecules were maintained. The box of water molecules in all systems contained around 13635 TIP3P water molecules. A 2 fs time step was used in all simulations, and long-range electrostatic interactions were treated with the particle mesh Ewald (PME) procedure with a 10 Å non-bonded cutoff. Bond lengths involving hydrogen atoms were constrained using the SHAKE algorithm. All systems were minimized prior to the production run. The minimization employed the SANDER module under constant volume conditions. The solvent molecules were first relaxed, while all heavy atoms in both protein and ATP were restrained with forces of 500 kcal mol^{-1} $angstrom^{-2}$. Then, the systems were continually relaxed. All heavy atoms of the system were restrained with forces of 500 kcal mol^{-1} $angstrom^{-2}$, except the atoms of the residues modeled by the Loop Search module of Sybyl6.8. Finally, all restraints were lifted and the whole system was relaxed. The three steps above all feature 1000 cycles of steepest descent followed by 1000 cycles of conjugate gradient minimization. After the relaxation, 300 ps of MD simulations were carried out at constant volume, with 10 kcal mol^{-1} $angstrom^{-2}$ restraint on solute. Then 5 ns of equilibration MD followed by 5 ns of production MD were respectively carried out on all systems at constant pressure (1 atm). All simulations were performed at 300 K.

Results and discussion

The root-mean-squared deviations (RMSD) value curves of backbone atoms during the production MD simulations have been obtained. The curves in Fig. 1 show that corresponding to the relaxation of the systems, the RMSD values of the backbone atoms of the complexes increase slowly before 600 ps, And after 600 ps, the RMSD values are fairly stable around 2 angstroms. The total potential

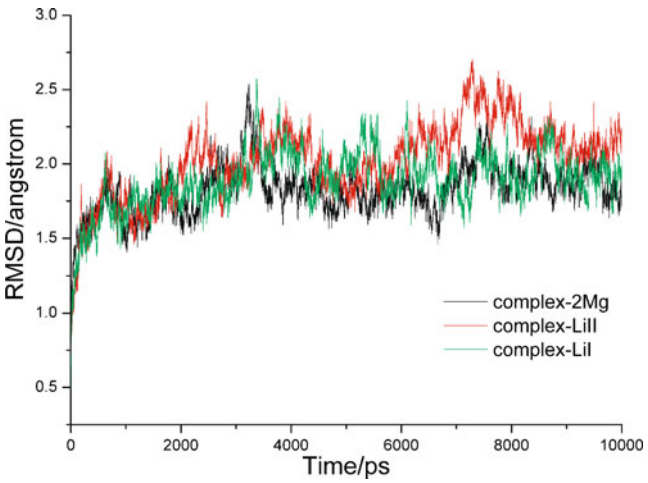

Fig. 1 RMSD value curves of backbone atoms during the production simulations

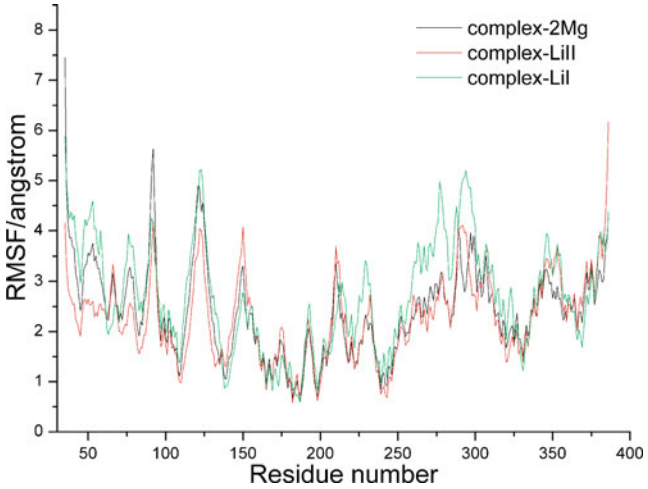

Fig. 2 Root mean square (RMS) fluctuation value curves of Cα atomic positions of all systems

energy fluctuates around a constant mean value after 1000 ps. This indicates the systems attain equilibrium.

RMS fluctuation (RMSF) values from structure provide an approach to evaluate the convergence of the dynamical properties of systems. As shown in Fig. 2, the fluctuation values of the complex-2 Mg (black curve) and the complex-LiII (red curve) are almost the same. Most fluctuation values of complex-LiI (green curves) are higher than that of complex-2 Mg and the complex-LiII, especially the values corresponding residues 260 to residues 300. This indicates that when Mg_I^{2+} is replaced by Li^+, the thermostability of the system will decrease.

As shown in Fig. 3a and b, when Mg_{II}^{2+} is replaced by Li^+, there is little change in the conformation of ATP. In the complex-LiII, the interactions between ATP and metal atoms are almost the same as that in the complex-2 Mg. The oxygen atoms $O^{3\gamma}$ and $O^{2\beta}$ of ATP still interact with Mg_I^{2+}, while the oxygen atoms $O^{2\alpha}$ and $O^{2\gamma}$ still interact with Li_{II}^{+}. In comparison, as shown in Fig. 3c, when Mg_I^{2+} is replaced by Li^+, there are some changes in the conformation of ATP. The oxygen atom $O^{2\beta}$ of ATP does not interact with Li_I^{+}, but with Mg_{II}^{2+} for the low electrostatic interaction between Li^+ and $O^{2\beta}$. The bond angles between γ- and β-P atoms of ATP and the oxygen atom between them in all systems were monitored. As shown in Fig. 4, the bond angles in complex-2 Mg and complex-LiII are both around 135 degrees while in complex-LiI the angle decreases by 10 degrees.

According to experimental studies on PKA, G-loop plays an essential role in catalytic reactions. It structurally guarantees the in-line phosphoryl transfer mechanism [18].

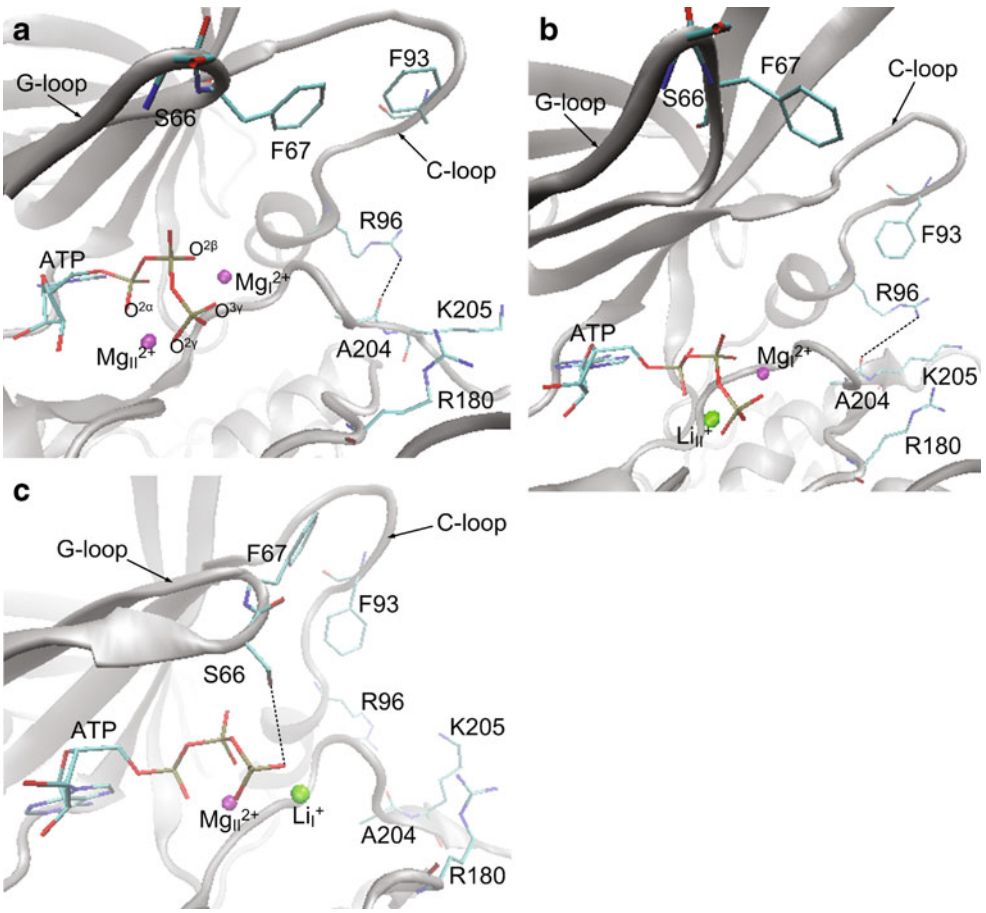

Fig. 3 Interactions in ATP binding site and substrate binding site of GSK. Molecules shown in stick model are ATP and residues in GSK; Atoms shown in ball model are metal ions in GSK, purple atoms are Mg^{2+}, green ones are Li^+. **a** shows the interaction details in complex-2 Mg; **b** shows the details in complex-LiII and **c** shows the details in complex-LiI

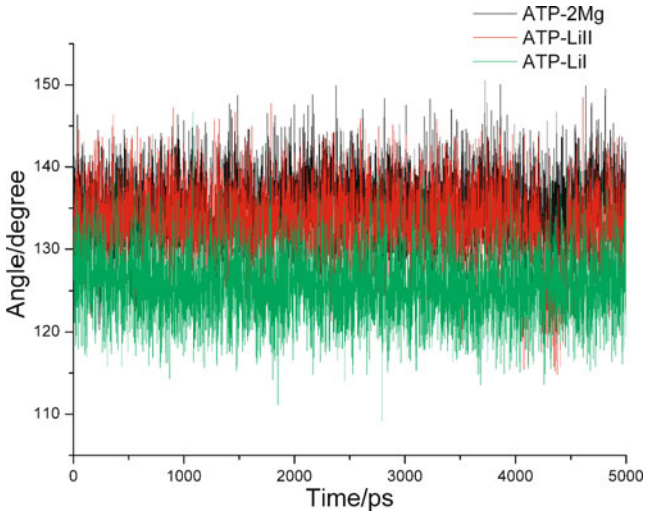

Fig. 4 Bond angles between γ- and β- P atoms of ATP and the oxygen atom between them

Mutations on G-loop can significantly reduce the affinity for ATP and lower the rate of phosphoryl transfer [19, 20]. Similar results have also been observed in studies on CDK [21, 22]. In our systems, when Mg_I^{2+} is replaced by Li^+, Ser66 of G-loop forms H-bond with the oxygen atom $O^{3\gamma}$ of ATP(occupation is 63.70%, refer to Table 1). The formation of the H-bond leads G-loop to cover ATP more tightly. Considering the changes it causes, we believe that the replacement of Mg_I^{2+} with Li^+ in GSK-3 can demolish in-line phosphoryl transfer mechanism and then reduce the rate of phosphoryl transfer.

Compared with CDK2, p38-γ, and ERK2, GSK-3β does not have the threonine phosphorylation site in the activation loop, thus Arg96 takes on an important role in GSK-3β. To align the two kinase domains, the substrate should be prephosphated. According to crystallography studies, the phospho-group of the substrate interacts with the positively charged residues Arg96, Arg180, and Lys205 just as the phospho-threonine in MAP kinases interacts with the positively charged residues [23–25]. Mutation studies have revealed that when Arg96 is mutated to Ala or Lys, GSK-3β lost its kinase activity [26], which further affirms the importance of Arg96.

Unlike in complex-2 Mg and complex-LiII, as shown in Fig. 3, the C-loop in complex-LiI adopts distorted conformations. The phenyl of Phe93 interaction with phenyl of Phe67 by hydrophobic interaction is destroyed. The distortion of C-loop induces the displacement of Arg96. The guanidino of Arg96 turns by about 90 degrees from Arg180, and cannot form H-bond with Ala204, refer to Table 1. This disturbs the conformations of phospho-group binding site formed by Arg96, Arg180 and Lys205, and probably could weaken the electrostatic interactions between the phospho-group of substrate and the three positively charged residues, and subsequently disturb the alignment of the two kinase domains and reduce the activity of GSK-3 eventually.

Conclusions

The effect of Li^+ on GSK-3β is illustrated by MD simulation. When Mg_I^{2+} is replaced by Li^+, the atom fluctuation of GSK-3 will rise. When Mg_{II}^{2+} is replaced by Li^+, there is little change in the conformation of ATP and the interactions between ATP and metal ions hardly change. When Mg_I^{2+} is replaced by Li^+, the oxygen atom $O^{2\beta}$ of ATP does not interacts with Li_I^+, but with Mg_{II}^{2+} for the low electrostatic interaction between Li^+ and $O^{2\beta}$. The bond angles between γ- and β- P atoms of ATP and the oxygen atom between them in complex-2 Mg and complex-LiII are both around 135 degrees while in complex-LiI the angle decreases by 10 degrees. The H-bond formation between Ser66 and the oxygen atom $O^{3\gamma}$ of ATP leads G-loop to cover ATP more tightly. Considering the changes it causes, we believe that the replacement of Mg_I^{2+} with Li^+ in GSK-3 can compromise in-line phosphoryl transfer mechanism. In addition, when Mg_I^{2+} is replaced with Li^+, the C-loop adopts distortional conformations. The guanidino of Arg96 turns by about 90 degrees from Arg180 and cannot form H-bond with Ala204, which may weaken the electrostatic interactions between the phospho-group of substrates and the three positively charged residues, and eventually reduce the activity of GSK-3. All the results we have observed above clearly suggest that the inhibition of GSK-3 is caused by the replacement of MgI with Li^+.

Table 1 Hydrogen bonds in the ATP binding site and the substrate binding site

Complex	Hydrogen bond	Distance (Å)	Angle (°)	Occupied (%)
Complex-2 Mg	(Ala204)O···HH1–NH1(Arg96)	2.91	22.01	66.92
	(ATP)$O^{3\gamma}$···HG–OG(Ser66)	–	–	–
Complex-LiII	(Ala204)O···HH1–NH1(Arg96)	2.96	24.78	13.16
	(ATP)$O^{3\gamma}$···HZ1–NZ(Ser66)	–	–	–
Complex-LiI	(Ala204)O···HH1–NH1(Arg96)	2.93	45.22	0.02
	(ATP)$O^{3\gamma}$···HZ2–NZ(Ser66)	2.73	14.86	63.70

Acknowledgments This work was supported by grants from National High Technology Research and Development Program of China (863 Program, 2007AA02Z301), Natural Science Foundation of China (No.20803063).

References

1. Embi N, Rylatt DB, Cohen P (1980) Eur J Biochem 107:519–527
2. Cross DA, Alessi DR, Cohen P, Andelkovich M, Hemmings BA (1995) Nature 378:785–789
3. Hoeflich KP, Luo J, Rubie EA, Tsao MS, Jin O, Woodgett JR (2000) Nature 406:86–90
4. Woodgett JR (1990) EMBO J 9:2431–2438
5. Zhang N, Jiang YJ, Zou JW, Zhuang SL, Jin HX, Yu QS (2007) Proteins 67:941–949
6. Zhang N, Jiang YJ, Zou JW, Zhang B, Wang YH, Yu QS (2006) Eur J Med Chem 41:373–378
7. Martinez A, Castro A, Medina M (2006) Glycogen Synthase Kinase 3 (GSK-3) and Its Inhibitors. Wiley, Hoboken, New Jersey
8. Jope RS, Johnson GV (2004) Trends Biochem Sci 29:95–102
9. Fiol CJ, Wang A, Roeske RW, Roach PJ (1990) J Biol Chem 265:6061–6065
10. Herberg FW, Doyle ML, Cox S, Taylor SS (1999) Biochemistry 38:6352–6360
11. Cade JFJ (1949) Med J Aust 2:349–352
12. Klein PS, Melton DA (1996) Proc Natl Acad Sci USA 93:8455–8459
13. Stambolic V, Ruel L, Woodgett JR (1996) Curr Biol 6:1664–1668
14. Davies SP, Reddy H, Caivano M, Cohen P (2000) Biochem J 351:95–105
15. Ryves WJ, Harwood AJ (2001) Biochem Biophys Res Commun 280:720–725
16. Ryves WJ, Dajani R, Pearl L, Harwood AJ (2002) Biochem Biophys Res Commun 290:967–972
17. http://www.pharmacy.manchester.ac.uk/bryce/amber
18. Jin HX, Wu TX, Jiang YJ, Zou JW, Zhuang SL, Mao X, Yu QS (2007) J Mol Struc (THEOCHEM) 805:9–15
19. Aimes RT, Hemmer W, Taylor SS (2000) Biochem 39:8325–8332
20. Grant B, Hemmer W, Tsigelny I, Adams JA, Taylor SS (1998) Biochem 37:7708–7715
21. Bártová I, Otyepka M, Kříž Z, Koča J (2005) Protein Sci 14:445–451
22. Bártová I, Otyepka M, KŘÍž Z, Koča J (2004) Protein Sci 13:1449–1457
23. ter Haar E, Coll JT, Austen DA, Hsiao HM, Swenson L, Jain J (2001) Nat Struct Biol 8:593–596
24. Dajani R, Fraser E, Roe SM, Young N, Good V, Dale TC, Pearl LH (2001) Cell 105:721–732
25. Dajani R, Fraser E, Roe SM, Yeo M, Good VM, Thompson V, Dale TC, Pearl LH (2003) EMBO J 22:494–501
26. Frame S, Cohen P, Biondi RM (2001) Mol Cell 7:1321–1327